NANO · MICRO small
www.small-journal.com

Quantum Dot–Based FRET Immunoassay for HER2 Using Ultrasmall Affinity Proteins

*Yu-Tang Wu, Xue Qiu, Sarah Lindbo, Kimihiro Susumu, Igor L. Medintz, Sophia Hober, and Niko Hildebrandt**

Engineered scaffold affinity proteins are used in many biological applications with the aim of replacing natural antibodies. Although their very small sizes are beneficial for multivalent nanoparticle conjugation and efficient Förster resonance energy transfer (FRET), the application of engineered affinity proteins in such nanobiosensing formats has been largely neglected. Here, it is shown that very small (≈6.5 kDa) histidine-tagged albumin-binding domain-derived affinity proteins (ADAPTs) can efficiently self-assemble to zwitterionic ligand–coated quantum dots (QDs). These ADAPT–QD conjugates are significantly smaller than QD-conjugates based on IgG, Fab', or single-domain antibodies. Immediate applicability by the quantification of the human epidermal growth factor receptor 2 (HER2) in serum-containing samples using time-gated Tb-to-QD FRET detection on the clinical benchtop immunoassay analyzer KRYPTOR is demonstrated here. Limits of detection down to 40×10^{-12} M (≈8 ng mL^{-1}) are in a relevant clinical concentration range and outperform previously tested assays with antibodies, antibody fragments, and nanobodies.

Immunoassays are dominated by the use of antibodies because of their broad accessibility and the fewer restrictions for biosensing in solution regarding size, structure, and environment.[1] However, the large sizes, complex structures, and relatively expensive and laborious production of IgG-based antibodies have led to the development of alternative affinity proteins.[2] Small single-domain antibodies (or nanobodies)[3] can be naturally produced or selected in vitro. Similarly, engineered scaffold proteins are selected in vitro and can either be produced in bacterial hosts or chemically synthesized. The most common synthetic binding proteins are (in alphabetical order) affibodies,[4] anticalins,[5] designed ankyrin repeat proteins,[6] and monobodies.[7] The main applications of these antibody alternatives are therapy, drug delivery, and in vivo and in vitro imaging.[7,8] However, these much smaller affinity binders would have significant advantages for bioassays based on Förster resonance energy transfer (FRET) and nanoparticles. The limited FRET distance of ≈10 nm[9] and the requirement of oriented and multivalent conjugation on nanoparticles,[10] in combination with their already relatively large sizes clearly favor the use of small biomolecules for biosensing. Surprisingly, only a few studies have reported the combination of synthesized scaffold proteins with FRET[11,12] or nanoparticles.[13,14] Semiconductor quantum dots (QDs) are important optical nanomaterials for immunoassays,[15–19] and exhibit unique properties for versatile FRET diagnostics.[20–25] Nanobodies have been conjugated to QDs[26,27] and applied for both FRET immunoassays[28,29] and FRET imaging[30] in combination with supramolecular terbium

Y.-T. Wu, Dr. X. Qiu, Prof. N. Hildebrandt
NanoBioPhotonics (nanofret.com)
Institute for Integrative Biology of the Cell
Université Paris-Saclay
Université Paris-Sud
CNRS
CEA
Orsay, France
E-mail: niko.hildebrandt@u-psud.fr

The ORCID identification number(s) for the author(s) of this article can be found under https://doi.org/10.1002/smll.201802266.

DOI: 10.1002/smll.201802266

Dr. S. Lindbo, Prof. S. Hober
Department of Protein Science
KTH – Royal Institute of Technology
Stockholm, Sweden

Dr. K. Susumu
Optical Sciences Division
Code 5600
U.S. Naval Research Laboratory
Washington, DC, USA

Dr. K. Susumu
KeyW Corporation
Hanover, MD 21076, USA

Dr. I. L. Medintz
Center for Bio/Molecular Science and Engineering
Code 6900
U.S. Naval Research Laboratory
Washington, DC, USA

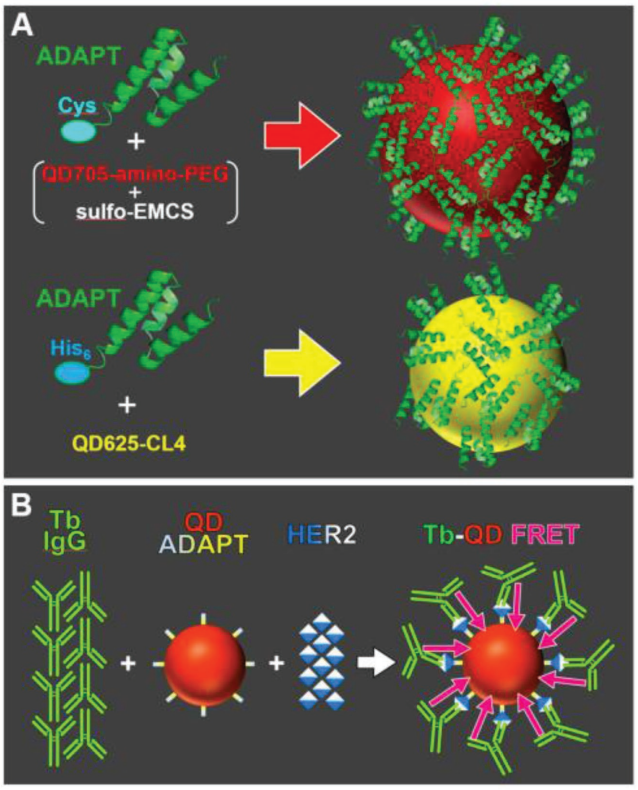

Figure 1. A) QD705 was conjugated with ADAPT6-Cys via a sulfhydryl reaction by adding sulfo-EMCS to introduce maleimide to the amino-PEG QD705 surface. QD625 was conjugated with ADAPT6-His_6 via Zn-His_6 self-assembly. B) Mixing of Tb-conjugated IgG (Pertuzumab), ADAPT-conjugated QDs, and soluble HER2 led to the formation of immunological sandwich complexes and a concomitant close proximity between Tb and QD, which, in turn, resulted in Tb-to-QD FRET for HER2 quantification.

(Tb) complexes[31] and time-gated (TG) detection.[32] The application and performance of even smaller engineered scaffold proteins in such QD-FRET immunosensors remains to be demonstrated.

Here, we show that a new class of very small (≈6.5 kDa; ≈1.0 × 1.5 × 2.5 nm^3) albumin-binding domain-derived affinity proteins (ADAPTs) against the human epidermal growth factor receptor 2 (HER2),[33,34] which have previously been used for in vivo radionuclide imaging of HER2 positive tumor xenografts,[35,36] can be applied for advanced Tb-to-QD FRET immunoassays. Specifically engineered anti-HER2-ADAPTs with histidine tags (His_6) or single cysteines (Cys) were used for conjugation to two different QDs emitting at 625 and 705 nm, respectively, whereas Tb were conjugated to Pertuzumab anti-HER2 antibodies (Genentech/Roche Diagnostics). TG-FRET sandwich immunoassays were performed on a clinical immunofluorescence plate reader (KRYPTOR, Thermo Fisher) in TRIS buffer containing 0.5% bovine serum albumin (BSA) and 10% serum. All detection limits were in a clinically relevant concentration range of soluble HER2 for breast cancer diagnostics (7–3000 ng mL^{-1})[37] and in the case of the ADAPT6-His_6-QD625 conjugates even below the clinical cutoff level of 15 ng mL^{-1} HER2.[37,38] The ADAPT6-His_6-QD625 also outperformed QD conjugates based on nanobodies, Fab' fragments, and

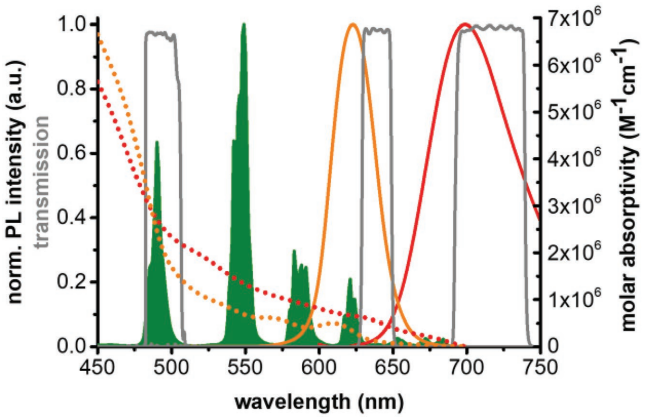

Figure 2. Absorption (dotted lines) and PL emission spectra of QD625 (orange) and QD705 (red), PL emission spectrum of Tb (green), and transmission spectra of the bandpass filters used for Tb and QD detection (gray). The absorption maximum of Tb is ≈339 nm (not shown).

IgG antibodies that were previously used in similar Tb-to-QD FRET immunoassays for HER2.[28]

To produce ADAPT–QD conjugates, we applied two different approaches (**Figure 1**A; see Supporting Information for experimental details) that we previously used to prepare various QD conjugates with antibodies and nanobodies. The first conjugation strategy attached histidine tag containing ADAPTs[33] by metal-affinity mediated self-assembly[26] to the Zn-rich surface of commercial QD625 (Qdot625, Thermo Fisher), coated with compact zwitterionic ligands (CL4).[39] This direct conjugation procedure allowed for a very close proximity between the QD surface and the anti-HER2-ADAPT. The second conjugation technique, attached cysteine (Cys) terminated ADAPTs to the amino-PEG coated surfaces of QD705 (Qdot705, Thermo Fisher) via a N-ε-maleimidocaproyl-oxysulfosuccinimide ester (sulfo-EMCS) crosslinker.[40] In contrast to the QD625-ADAPTs, the additional PEG coating on the QD705 placed the ADAPTs significantly further from the QD surface. The more than 1000-fold difference in extinction coefficients at 280 nm between the QDs and ADAPTs did not allow for a quantification of the exact number of ADAPTs per QD but an excess of ADAPTs per QD could be confirmed by the FRET immunoassays (vide infra). Taking into account a conjugation efficiency of close to unity for His_6-Zn self-assembly on QD surfaces, we assumed ≈20:1 ADAPT/QD625 labeling ratio. The large excess of ADAPT-Cys per QD705 (107:1) during conjugation and the larger size compared to the QD625 let us estimate an even higher number of ADAPTs per QD705. As we did not aim at systematically studying the valency of ADAPT molecules on QDs, an ADAPT-saturated QD surface (without knowing the exact number) was an adequate condition for our FRET immunoassays.

As the donor counterpart for the HER2 FRET immunoassays (Figure 1B), we used a full length IgG anti-HER2 antibody (Pertuzumab) that was conjugated with Lumi4-Tb.[28,41] Pertuzumab was used as Tb donor antibody since it recognizes a different epitope on HER2 than anti-HER2 ADAPT. Upon addition of HER2 containing samples to solutions of Tb and QD conjugates, both Tb–Pertuzumab and ADAPT–QD bound to HER2, which brought Tb and QD in close proximity and led

to FRET from Tb to QD after excitation of Tb (Figure 1B). As shown in **Figure 2**, the photoluminescence (PL) spectrum of Tb and the absorption spectra of both QDs overlap significantly, which resulted in Förster distances of R_0(Tb/QD625) = 9.7 nm and R_0(Tb/QD705) = 10.4 nm (see Supporting Information for determination). In addition to the larger R_0, the Tb-QD705 FRET pair also provided a spectrally broader detection of FRET-sensitized QD PL with significantly lower background PL from Tb (Figure 2). This usually results in higher sensitivity compared to Tb–QD FRET pairs with shorter QD PL wavelengths.[35] On the other hand, the CL4-coated QD625 allowed for a direct attachment of ADAPT and therefore a shorter distance to the QD surface and a higher FRET efficiency.

To evaluate the biosensing performance of the ADAPT–QD conjugates, we studied homogeneous Tb-to-QD FRET immunoassays for HER2 with both conjugates (ADAPT6-His_6-QD625 and ADAPT6-Cys-QD705). The ADAPT6 constructs had similar affinities to HER2 than Pertuzumab (K_D(ADAPT-His_6) = 1.3×10^{-9} M; K_D(ADAPT-Cys) = 4×10^{-9} M; K_D(Pertuzumab) = 1.9×10^{-9} M),[33,35,42] suggesting their suitability for sensitive detection of HER2 in FRET-based assays. The immunoassays were performed both in TRIS buffer containing 0.5% BSA and in TRIS buffer containing 0.5% BSA and 10% of serum, because initial experiments with 10%, 20%, and 30% of serum (Figure S2, Supporting Information) showed the best performance for 10%. Assay calibration curves (**Figure 3**) were acquired on a KRYPTOR compact PLUS, which simultaneously detected the time-gated (0.1–0.9 ms) PL intensities of Tb donor (I_{Tb}) and QD acceptor (I_{QD}).[28,32] The *FRET-ratio* = I_{QD}/I_{Tb} was used to determine HER2 concentrations. All assay curves showed a strong increase of *FRET-ratio* with increasing HER2 concentration from 0.075×10^{-9} M to ≈3×10^{-9} M, after which the curves started to level off and remained at an approximately constant *FRET-ratio* between 6×10^{-9} M and 12×10^{-9} M HER2. Such saturation is typical for homogeneous separation-free FRET immunoassays and is caused by the complete binding of one or both affinity binders (ADAPT or antibody) to the HER2 antigens. Fifty microliters of HER2 (3×10^{-9} M) were added to a 100 µL solution of 1.5×10^{-9} M Tb–Pertuzumab and 0.75×10^{-9} M ADAPT–QD (concentrations of Pertuzumab and QD, respectively). Thus, 3×10^{-9} M HER2 corresponded to 1×10^{-9} M in the measuring volume of 150 µL, which showed that the saturation was caused by the Tb–Pertuzumab concentration (1×10^{-9} M in 150 µL). It also confirmed the excess of ADAPT per QD, because the QD concentration was only 0.5×10^{-9} M in the 150 µL assay volume.

Although both types of ADAPT–QD assays could distinguish HER2 concentrations in clinically relevant concentrations for breast cancer diagnostics,[37,38] the slopes (sensitivity), the *FRET-ratio* saturation values of the calibration curves (Figure 3A), and the limits of detection (LODs, Figure 3B and **Table 1**) clearly show the superior performance of the ADAPT6-His_6-QD625. While 10% of serum inside the sample led to slightly higher LODs, they were still below the clinical cutoff level recommended for soluble HER2 (15 ng mL^{-1}).[37,38] The Tb–Pertuzumab–HER2-ADAPT-QD625 FRET assay also outperformed other affinity binder combinations including nanobodies, Fab' fragments, and IgGs.[28] Only a combination of V_HH nanobodies that were attached to QDs by a terminal cysteine

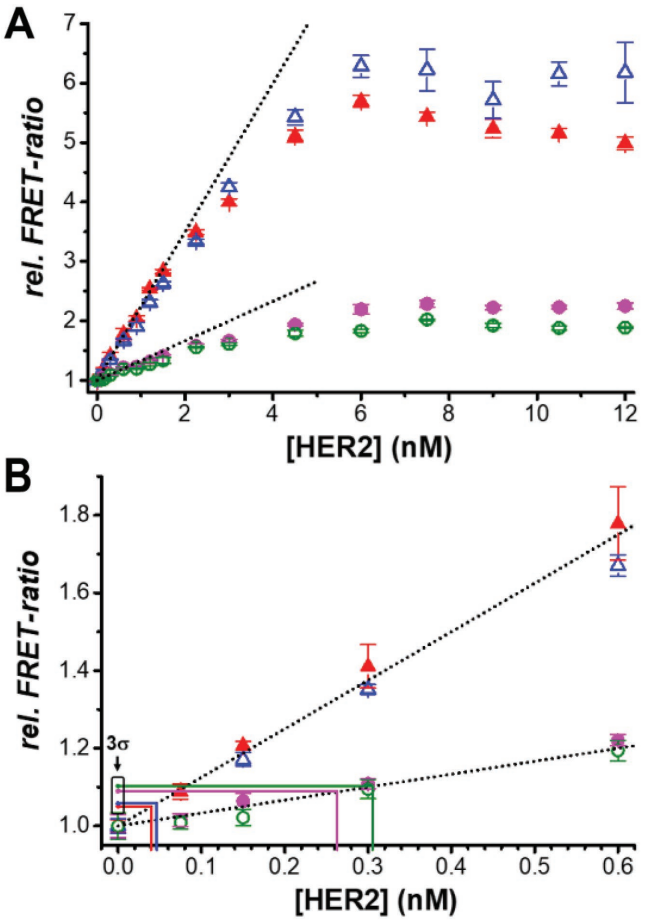

Figure 3. A) Calibration curves of Tb-to-QD FRET immunoassay for HER2 using ADAPT-His_6-QD625 (triangles; blue and red) and ADAPT-Cys-QD705 (circles; magenta and green). Concentrations correspond to HER2 in a 50 µL sample of TRIS buffer with 0.5% BSA and without serum (filled symbols; red and magenta) or with 10% of serum (open symbols; blue and green). Concentrations in a pure serum sample (5 µL within the 50 µL sample) would be tenfold higher. Dotted lines present the linearly increasing part of the calibration curves at low concentrations. B) Lower concentration range of the calibration curves from (A), which was used to estimate the LODs (3σ above zero). Error bars correspond to standard deviations (σ) with $n = 3$ for all HER2 containing samples and $n = 30$ for the zero-control (no HER2).

(oriented conjugation) showed similar LODs (Table 1) but only in buffer (addition of serum led to nonspecific binding). Our assays also provided lower LODs compared to QD-to-quencher (1×10^{-9} M) and QD-to-dye (12×10^{-9} M) FRET immunoassays for the vascular epidermal growth factor receptor (VEGF),[22] QD-to-gold nanoparticle FRET immunoassays for the hepatitis B surface antigen (HBsAg, 9 ng mL^{-1} or 380×10^{-12} M),[23] QD-to-dye FRET immunoassays for octachlorostyrene (OCT, 3.8×10^{-9} M),[24] and QD-to-dye or QD-to-quencher FRET immunoassays for 2,4,6-trinitrotoluene (TNT, 20 ng mL^{-1} or 90×10^{-9} M).[25] Only amplified QD–based immunoassays resulted in significantly lower LODs for prostate specific antigen (PSA, 1.8 pg mL^{-1} or 60 fM)[19] or VEGF (5×10^{-12} M).[22] Commercial enzyme-linked immunosorbent assays (ELISAs) for HER2 advertise LODs down to a few pg mL^{-1}

Table 1. LODs for HER2 in 50 µL samples using combinations of different engineered and natural affinity proteins (ADAPT, V_HH nanobodies, Fab' fragments, and IgG).

Current work	LOD ($\times 10^{-9}$ M)	LOD (ng mL^{-1})
Tb-IgG/ADAPT-His_6-QD625	0.04 ± 0.01	8 ± 2
Tb-IgG/ADAPT-His_6-QD625 10% serum*	0.05 ± 0.01	10 ± 2
Tb-IgG/ADAPT-Cys-QD705	0.30 ± 0.02	50 ± 4
Tb-IgG/ADAPT-Cys-QD705 10% serum*	0.30 ± 0.03	60 ± 6
LODs in previous work[28] (only buffer)		
Tb-IgG/IgG-QD650: 0.09×10^{-9} M	Tb-V_HH/V_HH-QD650 (oriented): 0.05×10^{-9} M	
Tb-IgG/IgG-QD605: 0.15×10^{-9} M	Tb-V_HH/V_HH-QD650 (random): 0.08×10^{-9} M	
Tb-IgG/Fab'-QD650: 0.11×10^{-9} M	Tb-V_HH/V_HH-QD605 (oriented): 0.04×10^{-9} M	
Tb-IgG/Fab'-QD605: 0.12×10^{-9} M	Tb-V_HH/V_HH-QD605 (random): 0.12×10^{-9} M	

*Concentrations of LODs correspond to those in the 50 µL samples that contain 5 µL of serum. Therefore, LODs in a serum sample would be tenfold higher.

(e.g., Aviscera Bioscience), but these assays are heterogeneous and therefore more time and labor consuming than our homogeneous assays. By optimization of the ADAPT-His_6-QD conjugation, e.g., by a detailed investigation of different numbers of ADAPT per QD,[43] or multiplexing with different QDs,[44] further improvement of the performance and versatility of the ADAPT–QD conjugates for biosensing should be possible.

In conclusion, we have demonstrated that small engineered affinity proteins, namely ADAPTs with an approximate molecular weight of 6.5 kDa, can be efficiently self-assembled to 625 nm emitting QDs via histidine tags and that these ADAPT–QD conjugates can be applied for highly sensitive FRET immunoassays for HER2. This new nanobiomaterial combination showed an improved FRET assay performance compared to QD conjugates with antibodies, antibody fragments, or nanobodies and may become a useful tool for many other optical biosensing and clinical applications in both spectroscopy and imaging. We also showed an alternative conjugation approach of cysteine-terminated ADAPTs through labeling to amino-PEG coated QDs via sulfo-EMCS crosslinkers. Although the detection limits were higher for this conjugate, our results demonstrated the versatility of ADAPT-conjugation to nanoparticles and the application to another QD color (emitting at 705 nm) showed the general possibility of color multiplexing. Our future efforts will be directed to further sensitivity optimization, the implementation of ADAPT–QD conjugates for different biomarkers, and the multiplexed detection of different analytes from single samples by different QD acceptors. Our proof-of-concept study showed the benefits of combining small affinity binders with QDs for improved FRET biosensing and we believe that, with the development of ADAPTs against various biomarkers, this nanoaffinity concept can become a very versatile and practical tool for FRET biosensing and other bioanalytical and clinical applications.

Supporting Information

Supporting Information is available from the Wiley Online Library or from the author.

Acknowledgements

The authors thank Lumiphore, Inc. for the gift of Lumi4 reagents. This work was partially funded by the European Commission (H2020-FET-Open project PROSEQO) and the Agence National de la Recherche (ANR) France (ANR projects NEUTRINOS, NANOHYPE, and AMPLIFY). Y.T.W. acknowledges the Taiwanese Ministry of Education and Université Paris-Sud for her PhD fellowship. I.M. acknowledges ONR, NRL, the NRL-Nanosciences Institute, and a LUCI grant in support of the VBFF program through the OSD. N.H. acknowledges the Institut Universitaire de France (IUF) for financial support.

Conflict of Interest

The authors declare no conflict of interest.

Keywords

ADAPT, HER2, nanoparticle, nonantibody scaffold, terbium

Received: June 13, 2018
Revised: July 2, 2018
Published online: August 5, 2018

[1] D. Wild, *The Immunoassay Handbook*, 4th ed., Elsevier, Amsterdam **2013**.
[2] R. N. Gilbreth, S. Koide, *Curr. Opin. Struct. Biol.* **2012**, *22*, 413.
[3] S. Muyldermans, in *Annual Review of Biochemistry*, Vol. *82*, (Ed: R. D. Kornberg), Annual Reviews, Palo Alto, **2013**, pp. 775–797.
[4] J. Löfblom, J. Feldwisch, V. Tolmachev, J. Carlsson, S. Stahl, F. Y. Frejd, *FEBS Lett.* **2010**, *584*, 2670.
[5] A. Richter, E. Eggenstein, A. Skerra, *FEBS Lett.* **2014**, *588*, 213.
[6] A. Plückthun, in *Annual Review of Pharmacology and Toxicology*, Vol. *55*, (Ed: P. A. Insel), Annual Reviews, Palo Alto, **2015**, pp. 489–511.
[7] F. Sha, G. Salzman, A. Gupta, S. Koide, *Protein Sci.* **2017**, *26*, 910.
[8] D. Schumacher, J. Helma, A. F. L. Schneider, H. Leonhardt, C. P. R. Hackenberger, *Angew. Chem., Int. Ed.* **2018**, *57*, 2314.
[9] I. L. Medintz, N. Hildebrandt, *FRET – Förster Resonance Energy Transfer. From Theory to Applications*, Wiley-VCH, Weinheim, Germany **2014**.
[10] K. E. Sapsford, W. R. Algar, L. Berti, K. B. Gemmill, B. J. Casey, E. Oh, M. H. Stewart, I. L. Medintz, *Chem. Rev.* **2013**, *113*, 1904.
[11] P. Limsakul, Q. Peng, Y. Q. Wu, M. E. Allen, J. Liang, A. G. Remacle, T. Lopez, X. Ge, B. K. Kay, H. M. Zhao, A. Y. Strongin, X. L. Yang, S. Y. Lu, Y. X. Wang, *Cell Chem. Biol.* **2018**, *25*,370.
[12] B. Renberg, P. A. Nygren, M. Eklund, A. E. Karlstrom, *Anal. Biochem.* **2004**, *334*, 72.
[13] J. H. Gao, K. Chen, Z. Miao, G. Ren, X. Y. Chen, S. S. Gambhir, Z. Cheng, *Biomaterials* **2011**, *32*, 2141.
[14] K. L. Gurunatha, A. C. Fournier, A. Urvoas, M. Valerio-Lepiniec, V. Marchi, P. Minard, E. Dujardin, *ACS Nano* **2016**, *10*, 3176.
[15] J. Shu, D. P. Tang, *Chem. - Asian J.* **2017**, *12*, 2780.
[16] Z. L. Qiu, J. Shu, D. P. Tang, *Anal. Chem.* **2017**, *89*, 5152.

[17] Y. X. Lin, Q. Zhou, D. P. Tang, R. Niessner, D. Knopp, *Anal. Chem.* **2017**, *89*, 5637.
[18] S. Z. Lv, K. Y. Zhang, Y. Y. Zeng, D. P. Tang, *Anal. Chem.* **2018**, *90*, 7086.
[19] K. Y. Zhang, S. Z. Lv, Z. Z. Lin, M. J. Li, D. P. Tang, *Biosens. Bioelectron.* **2018**, *101*, 159.
[20] D. Geißler, N. Hildebrandt, *Anal. Bioanal. Chem.* **2016**, *408*, 4475.
[21] N. Hildebrandt, C. M. Spillmann, W. R. Algar, T. Pons, M. H. Stewart, E. Oh, K. Susumu, S. A. Diaz, J. B. Delehanty, I. L. Medintz, *Chem. Rev.* **2017**, *117*, 536.
[22] R. Freeman, J. Girsh, A. F. J. Jou, J. A. A. Ho, T. Hug, J. Dernedde, I. Willner, *Anal. Chem.* **2012**, *84*, 6192.
[23] Q. H. Zeng, Y. L. Zhang, X. M. Liu, L. P. Tu, X. G. Kong, H. Zhang, *Chem. Commun.* **2012**, *48*, 1781.
[24] X. Wang, P. T. Sheng, L. P. Zhou, X. Tong, L. Shi, Q. Y. Cai, *Biosens. Bioelectron.* **2014**, *60*, 52.
[25] E. R. Goldman, I. L. Medintz, J. L. Whitley, A. Hayhurst, A. R. Clapp, H. T. Uyeda, J. R. Deschamps, M. E. Lassman, H. Mattoussi, *J. Am. Chem. Soc.* **2005**, *127*, 6744.
[26] K. Boeneman Gemmill, J. R. Deschamps, J. B. Delehanty, K. Susumu, M. H. Stewart, R. H. Glaven, G. P. Anderson, E. R. Goldman, A. L. Huston, I. L. Medintz, *Bioconjugate Chem.* **2013**, *24*, 269.
[27] A. Sukhanova, K. Even-Desrumeaux, A. Kisserli, T. Tabary, B. Reveil, J. M. Millot, P. Chames, D. Baty, M. Artemyev, V. Oleinikov, M. Pluot, J. H. M. Cohen, I. Nabiev, *Nanomedicine* **2012**, *8*, 516.
[28] X. Qiu, K. D. Wegner, Y. T. Wu, P. Henegouwen, T. L. Jennings, N. Hildebrandt, *Chem. Mater.* **2016**, *28*, 8256.
[29] K. D. Wegner, S. Linden, Z. W. Jin, T. L. Jennings, R. el Khoulati, P. Henegouwen, N. Hildebrandt, *Small* **2014**, *10*, 734.
[30] H. S. Afsari, M. C. Dos Santos, S. Linden, T. Chen, X. Qiu, P. Henegouwen, T. L. Jennings, K. Susumu, I. L. Medintz, N. Hildebrandt, L. W. Miller, *Sci. Adv.* **2016**, *2*, e1600265.
[31] N. Hildebrandt, K. D. Wegner, W. R. Algar, *Coord. Chem. Rev.* **2014**, *273–274*, 125.
[32] J. M. Zwier, N. Hildebrandt, in *Reviews in Fluorescence 2016* (Ed: C. D. Geddes), Springer International Publishing, **2017**, pp. 17–43.
[33] S. Lindbo, J. Garousi, M. Astrand, H. Honarvar, A. Orlova, S. Hober, V. Tolmachev, *Bioconjugate Chem.* **2016**, *27*, 716.
[34] J. Nilvebrant, M. Astrand, M. Georgieva-Kotseva, M. Bjoernmalm, J. Lofblom, S. Hober, *PLoS ONE* **2014**, *9*, e103094.
[35] J. Garousi, S. Lindbo, B. Mitran, J. Buijs, A. Vorobyeva, A. Orlova, V. Tolmachev, S. Hober, *Sci. Rep.* **2017**, *7*, 14780.
[36] J. Garousi, S. Lindbo, J. Nilvebrant, M. Astrand, J. Buijs, M. Sandstrom, H. Honarvar, A. Orlova, V. Tolmachev, S. Hober, *Cancer Res.* **2015**, *75*, 4364.
[37] V. Müller, I. Witzel, K. Pantel, S. Krenkel, H. J. Lück, R. Neumann, T. Keller, I. Dittmer, F. Jänicke, C. Thomssen, *Anticancer Res.* **2006**, *26*, 1479.
[38] K. S. Asgeirsson, A. Agrawal, C. Allen, A. Hitch, I. O. Ellis, C. Chapman, K. L. Cheung, J. F. R. Robertson, *Breast Cancer Res.* **2007**, *9*, R75, 8 pages.
[39] K. Susumu, E. Oh, J. B. Delehanty, J. B. Blanco-Canosa, B. J. Johnson, V. Jain, W. J. Hervey, W. R. Algar, K. Boeneman, P. E. Dawson, I. L. Medintz, *J. Am. Chem. Soc.* **2011**, *133*, 9480.
[40] S. Bhuckory, O. Lefebvre, X. Qiu, K. D. Wegner, N. Hildebrandt, *Sensors* **2016**, *16*, 197.
[41] J. Xu, T. M. Corneillie, E. G. Moore, G.-L. Law, N. G. Butlin, K. N. Raymond, *J. Am. Chem. Soc.* **2011**, *133*, 19900.
[42] W. Y. Fu, Y. X. Wang, Y. S. Zhang, L. J. Xiong, H. Takeda, L. Ding, Q. F. Xu, L. D. He, W. L. Tan, A. N. Bethune, L. J. Zhou, *mAbs* **2014**, *6*, 978.
[43] G. Annio, T. L. Jennings, O. Tagit, N. Hildebrandt, *Bioconjugate Chem.* **2018**, *29*, 2082.
[44] D. Geissler, L. J. Charbonniere, R. F. Ziessel, N. G. Butlin, H.-G. Löhmannsröben, N. Hildebrandt, *Angew. Chem., Int. Ed.* **2010**, *49*, 1396.